Evaluating Smartphone Accuracy for LTE Power Measurement

Yanis BOUSSAD
yanis.boussad@inria.fr
Université Côte d'Azur, Inria
Valbonne, France

M. Naoufal Mahfoudi
m1mahfoudi@eng.ucsd.edu
University of California San Diego
US

Arnaud Legout
arnaud.legout@inria.fr
Université Côte d'Azur, Inria
Valbonne, France

Leonardo Lizzi
leonardo.lizzi@unice.fr
Université Côte d'Azur, CNRS, LEAT
Biot, France

Fabien Ferrero
fabien.ferrero@unice.fr
Université Côte d'Azur, CNRS, LEAT
Biot, France

Walid Dabbous
walid.dabbous@inria.fr
Université Côte d'Azur, Inria
Valbonne, France

ABSTRACT

Smartphones are today relatively cheap devices that embed a large variety of sensors such as magnetometers or orientation sensors, but also the hardware to connect to most wireless communication technologies such as Wi-Fi, Bluetooth, or cellular networks. For this reason, companies, such as OpenSignal [23] or Tutela [30] use smartphones to make crowd-based measurements of the received power from the cellular infrastructure to help operators manage their infrastructure. However, to the best of our knowledge, the accuracy of such measurements has never been rigorously assessed.

The goal of this paper is to assess how accurate are measurements of received power from a 4G (LTE) antenna when performed from a Commercial Off-The-Shelf (COTS) smartphone in different environments. We first evaluate the granularity and limitations of the Android API that returns the received power. We explore how reliable are the measurements from a mono-polarized antenna in a fully controlled environment. We show that the orientation of the smartphone, the position of the source, and the distance to the source has a significant impact on the accuracy of the measurements. We introduce several calibration techniques based on radiation matrices manipulations and machine learning to calibrate the measurements, that is, to improve the accuracy to less than 5 dBm RMSE compared to a professional equipment. Finally, we explore how reliable are measurements in an outdoor environment, in the context of a multi-polarized antenna.

1 INTRODUCTION

Smartphones are sophisticated devices with a lot of embedded sensors, but also with the support of several wireless technologies, such are Wi-Fi, Bluetooth, 2G, 3G, 4G, and now 5G. For this reason, they are used to make measurements of received powers.

Such measurements are important in multiple contexts. We discuss a few such important practical contexts in the following. First, companies such as OpenSignal [23] or Tutela [30] make crowd-based cellular measurements that they sell to cellular operators to improve their network. Indeed, the received power as experienced by the consumers is key to understand the coverage of the cellular network and to decide where to place additional cells. Operators also use this information to have a better understanding of the competition. Second, large European projects, such as EMF-NET [24], Interphone [15], or GERoNiMO [25] explored the impact the exposure to electromagnetic fields on health. In particular, the Interphone study [15] is at the origin of the classification of the radiofrequency EMF as carcinogenic 2B by the World Health Organization [5]. However, all their studies faced the difficulty to accurately quantify the exposure of the population to radio-frequencies electromagnetic fields. For this reason, the European project COMOS [28] developed an Android app called XMobisense [4] to measure the exposure of a cohort during an experiment. This app had a confidential usage and is no more maintained. The ElectroSmart project [13] also developed an Android application to inform the general audience of their exposure. This project is still active and has more than 100k monthly users. Third, indoor positioning is an important problem. One approach to address this problem is to use Bluetooth beacons. In that context, the accurate estimation of the received power is important to determine the proximity to the surrounding beacons [31].

Whereas, the accuracy of the received power measurements is key to all these context, this is a surprisingly difficult problem and, to the best of our knowledge, there is no rigorous evaluation of this accuracy for COTS smartphones.

In this work, we evaluate the accuracy of an Android COTS smartphone to make measurements of the received power emitted from a 4G (LTE) antenna. Our contributions are the following. i) We evaluate the granularity and limitations of the Android API that provides the Received Signal Strength Indicator (RSSI) for a 4G signal. We show that not all methods to access the RSSI are equivalent on Android and that we can expect a 2 dBm granularity and an update at most every second for the measurements. ii) We explore the accuracy of the RSSI measurement in a fully controlled environment with a mono-polarized antenna. We show that the accuracy of the measures is extremely sensitive to the device orientation, source positioning, and distance to the source. iii) We propose several calibration techniques to improve the accuracy that relies on manipulations of radiation matrices and on machine learning. We show that we can significantly improve the accuracy and obtain a 5 dBm RMSE compared to a calibrated professional equipment. iv) We explore the accuracy of the RSSI measurement with a multi-polarized outdoor antenna. We show that the RSSI accuracy is far less sensitive to the device orientation due to the multi-polarization of the antenna and the MIMO capabilities of the device. v) All the calibration artifacts and measurements data are available to the community. The pre-computed calibration matrices are available as an Android mobile application for an easier reusability[1].

[1] All contributions will be given for the camera-ready version of the paper.

Previous works explored the possibility to perform measurements of the received power, but not for COTS devices with no additional dedicated hardware. Tan et al. proposed *Snoopy* [32], a spectrum analyzer that uses commodity Wi-Fi cards with frequency translators to sense a wide range of frequencies. The Wi-Fi card normally scans only at 2.4 GHz and 5 GHz. To extend this range and scan a wider spectrum, Snoopy uses an RF frequency translator that senses and translates the signals to adapt them to the supported frequency by the Wi-Fi card. This is not readily applicable to COTS smartphones as they do not expose RF connectors of their Wi-Fi cards. Another work that aimed at using commodity smartphone as a spectrum analyzer is presented by Ana et al. [21]. They used a portable Software Defined Radio (RTL-SDR) dongle that senses a continuous spectrum range from 52MHz to 2200 MHz, which they connect to a smartphone through USB. The dongle is the spectrum analyzer. The smartphone only processes the data from the dongle. In contrast to the two aforementioned works that rely on external hardware, CrowdREM [2] relies only on smartphones for spectrum analysis. The authors used an open-source mobile phone (OpenMoko [26]) on which they installed a modified Linux system and replaced the whole baseband system by OsmocomBB [27], another open-source GSM baseband implementation. They showed that smartphone accuracy is within 3 dBm while the device is still, but very sensitive to orientation with respect to the source, up to 10 dB difference.

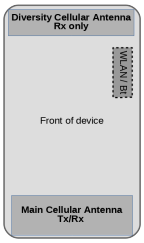

Figure 1: Location of antennas on a smartphone.

As opposed to the previous works, the solution we propose in this paper relies solely on a smartphone without any other external hardware. Moreover, our solution requires neither a hardware modification nor software modification (no rooting and no custom operating system required) on the smartphone. We mitigate the inaccuracy of smartphones [2] with a calibration algorithm that uses the Inertial Measurements Units (IMUs) of the mobile device to determine the correction power offset to apply.

The rest of the paper is organized as follows. In Section 2, we present some constraints affecting the design and placement of smartphone antennas and how this could impact the performances of these antennas. In Section 3, we present our methodology to make an experimental setup using open-source software. In Section 4, we show the effect of changing the smartphone orientation on the accuracy of the received power measurements. Next, we present a calibration algorithm in Section 5 that will correct the raw power measurements of the smartphone by compensating for the effect of orientation. In Section 6, we evaluate our algorithm in different scenarios, and in Section 7 we evaluate the reception performance of a smartphone with a multi-polarized antenna in an outdoor environment. We conclude the paper in Section 8.

2 SMARTPHONE ANTENNAS

Smartphones support various telecommunication protocols such as cellular technologies (GSM, WCDMA, LTE), Wi-Fi and Bluetooth. All these protocols usually work at different radio frequencies, spanning from 800 MHz up to 5 GHz [16]. In order to support the aforementioned telecommunication protocols, different antennas are required on the device. A dedicated antenna for Wi-Fi, one for Bluetooth, one for both GSM and WCDMA, and multiple antennas for LTE. It is common to have multiple technologies working at the same time like streaming music to your Bluetooth headset while downloading a file using cellular data. This can cause a lot of interference between the antennas. For this reason, smartphone manufacturers tend to limit the number of antennas by making multiband antennas that can be shared by more than one technology, like for example Bluetooth and Wi-Fi since they work on almost the same frequencies (around 2.4 GHz) [18]. Moreover, the design of an antenna depends mostly on the frequencies it will support. Antenna size is inversely proportional to the frequency: the lower the frequency, the bigger the antenna size. But the space constraints on modern smartphones makes it harder to fit all these antennas inside. Also, smartphone manufacturers are obliged to design their antennas in such a way to limit the radiated power when transmitting. This is known as the Specific Absorption Rate (SAR) [16]. SAR defines the maximum power the antenna should not exceed in order to not cause biological damage when the device is put very close to the human body. That's why the transmitting antennas are generally put at the bottom of the device, further from the head while the receive-only antennas or diversity antennas are generally on the upper part. Most of the smartphone manufacturers adopt the scheme depicted in Figure 1 for antennas placement.

Given all these design constraints, the architecture and the design of smartphone antennas will surely have an impact on their performances, as shown by Achtzehn et al [2], where the received signal power is easily affected by the device orientation. To verify this, we collected the reception pattern of an LG Nexus 5x cellular antennas along 3 axis inside an anechoic chamber (the detailed methodology is presented in section 3). The results are shown in Figure 2. As we can see, the received power changes depending on the orientation of the device and the polarization of the source (horizontal or vertical). Also, we notice the duality between the reception patterns for the two polarizations. When the reception is optimal for a given polarization, the other gives a lower performance. This may not always be the case as the reception performance depends on the antenna design and its symmetry with respect to the polarization axis.

3 METHODOLOGY

3.1 Experimental setup

We make an experimental setup for wireless cellular experimentation based on commodity hardware and open-source software. The framework allows signal generation and device testing.

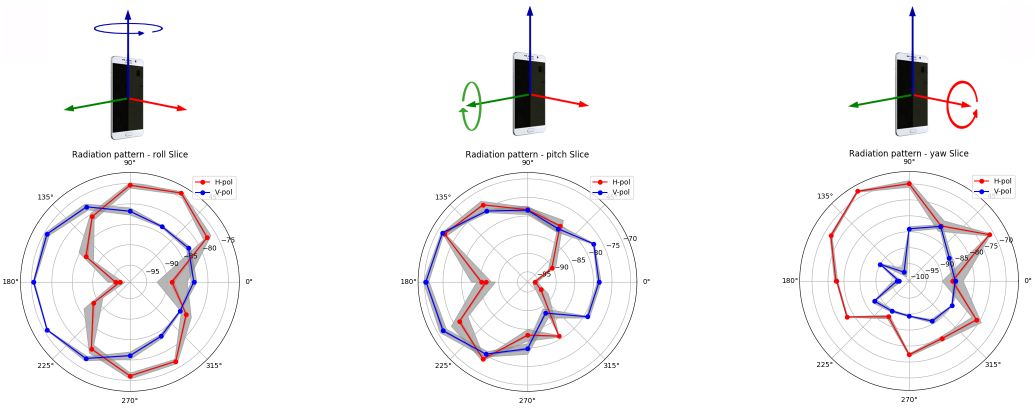

Figure 2: Reception pattern of the LG Nexus 5x in 3 planes: roll, pitch and yaw.

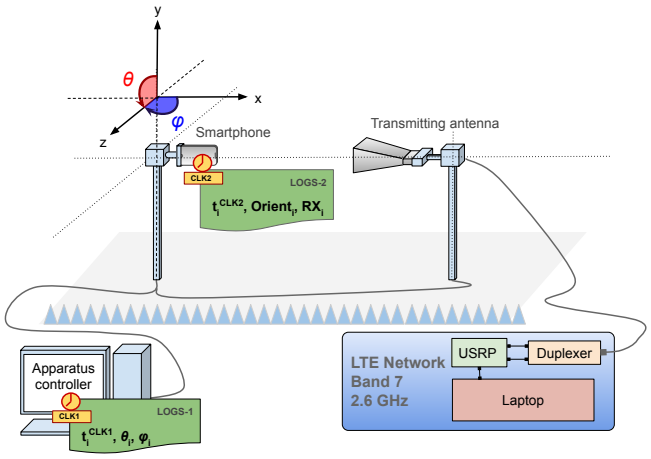

Figure 3: The experimental setup. We first measure the reference power using a spectrum analyzer, then we compare it with the raw measurements obtained from a COTS smartphone at 684 different orientations by rotating it along two axis φ and θ: φ makes 180 degrees rotation at a step of 10 degrees, for each value of φ, we change θ from 0 to 350 degrees at a step of 10 degrees.

3.1.1 Cellular signal generation. Instead of using specialized hardware for generating cellular network signal, we use OpenAirInterface (OAI) [22], an open-source, complete, software implementation of an LTE cellular network that can run on general-purpose processors. It is a cheap and working alternative for cellular network experimentation. We proceed as follows to generate the signal. The Core Network (CN) and the Radio Access Network (RAN) components of OAI usually run on two different machines to ensure real-time performances. To reduce the deployment costs of our setup, mobile data should be deactivated which will considerably reduce the computing load on the processor. Hence, both the CN and RAN components can run on the same machine. We use an HP Zbook laptop running Ubuntu 16.04 LTS with Intel i7-6th-gen processor and 32 GB of RAM. We connected the laptop to an Ettus B210 [14] Universal Software Radio Peripheral (USRP). A band 7 duplexer is used to connect both the RX and TX channels of the USRP to an ETS-Lindgren's 3115 double-ridged horn RX/TX antenna. It is a directional antenna with linear polarization having a gain of 10 dB at 2.5 GHz, and supporting a wide range of frequencies ranging from 750 MHz to 18 GHz. In our setup, it is called the source or the transmitting antenna, as shown in Figure 3.

3.1.2 Device Under Test. For the device under test, we use a Nexus 5X smartphone running Android 7. In order to attach the smartphone to the network, we program a SIM card with the necessary authentication parameters that we defined beforehand in the database of OAI. This allows the smartphone to discover and attach to the network.

3.1.3 Controlled environment with programmable robotic apparatus. We perform our experimentation in an anechoic chamber that has programmable robotic equipment both at the transmission and the reception sides. As shown in Figure 3, the reception platform is a two-axis positioning system that rotates along two axis: φ (Azimuth, the angle between x and z axes) and θ (Roll, the angle between y and z axes). φ can rotate 180 degrees (from -90 to +90) whereas θ can make 360-degrees rotation. The transmission platform (on the right of Figure 3) can only rotate along θ. It is located at φ=0. By combining the two-axis rotations, we can obtain measurements of the received power of the smartphone in different orientations in space. The reception and transmission are separated by a distance of 4 meters.

The two platforms are connected to a controller system (Apparatus controller) outside of the chamber that allows us to program the rotation of the platforms by defining the rotation range, the step, and the time duration it remains at each orientation. The apparatus controller is a Windows machine.

3.2 Measurement logs

We log the measurements at two levels. At the apparatus controller level (*LOGS-1*) , and at the smartphone level (*LOGS-2*). The logs are timestamped with the local clock, as illustrated in Figure 3.

For the smartphone log collections, we use an Android mobile application [20] dedicated to measuring the radiations emitted by

telecommunication infrastructures. It can measure all cellular technologies (GSM, WCDMA, and LTE) in addition to Bluetooth and Wi-Fi signals. It makes use of Android API calls to communicate with the smartphone baseband and the orientation sensors to take measurements of the received power and the device's orientation in space, respectively. We instrumented the application to collect the logs every 1 second. The logs are written in a single text file and saved on the device's local storage.

The apparatus controller creates timestamped logs of the values of its axes of rotation each time it reaches a programmed orientation. The logs are saved in text files on the apparatus controller desktop.

The clocks CLK1 and CLK2 at both levels should be synchronized before starting any experiment.

3.3 Logs processing

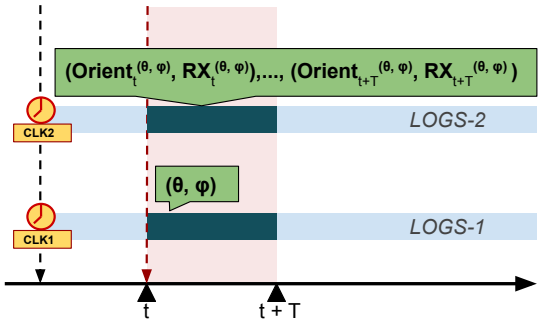

Figure 4: Log processing. From the smartphone logs (LOGS-2), we extract the orientation obtained from the orientation sensors, and the received power for the whole duration the smartphone remains in the orientation defined by (θ, φ)

We extract all the log files (*LOGS-1* and *LOGS-2*) from their respective locations, and we process them using a python script. We align the logs according to their timestamps as illustrated in Figure 4. At the beginning of each experiment, the apparatus makes a transitory rotation of its axes to reach the first programmed orientation. During this transitory period, the smartphone's received power keeps changing and stabilizes when the apparatus reaches the first programmed orientation. Since we keep the smartphone at the same orientation for T=10 seconds, The received power should remain stable for this whole duration until the apparatus starts to rotate to another orientation. We exploit this change and stabilization of the received power to pinpoint the corresponding change in orientation and be able to align the logs regardless of any possible desynchronization of CLK1 and CLK2. So for a given timestamp t from the apparatus logs (*LOGS-1*) indicating that the apparatus has reached a new orientation defined by (θ, φ), we extract the measurements from *LOGS-2*, starting from this timestamp t until the apparatus starts to change to another orientation (timestamp $t + T$), as depicted in Figure 4.

3.4 Type of logs

The logs collected at the apparatus controller are the coordinates of the axis of the reception platform. They are given in terms of φ and θ in degrees.

The received power in the case of LTE signal can be expressed in two different values, RSSI and RSRP. The RSSI is a general metric for wireless signals. The RSRP is only defined for LTE network. Both metrics express the received power, but they are computed differently. According to the definitions given by ETSI [1], Reference signal received power (RSRP), is the average power of the resource elements that carry cell-specific reference signals within the measurement bandwidth. The RSSI is the total power the smartphone observes across the whole band, including the main signal and co-channel non-serving cell signal, adjacent channel interference and even the thermal noise within the specified band. So RSRP is computed after demodulation, RSSI doesn't require demodulating the signal. That's why the RSRP is always less than the RSSI. The RSSI can take values from -51 dBm to -113 dBm. The RSRP can go from -140 dBm up to -43 dBm. We consider only the RSSI because it's easily measurable with a spectrum analyzer without the need to demodulate the signal.

The smartphone logs contain both the received power expressed as RSSI, in addition to the device orientation in space as expressed as quaternions.

3.4.1 Getting the received power on Android. The Android Application Programming Interfaces (APIs) offer two possibilities to get the received power by the device. One method consists of registering a listener that will generate a callback whenever there is a change in the signal strength. The other one is an explicit request to the operating system to retrieve the received power (or signal strength). We detail them in the following.

• *PhoneStateListener.* : is a callback-based methods available on Android under the *telephony* package to monitor the signal strength, that require registering a listener for specific events (for example, changes in the signal strength). So by registering a listener to monitor the changes in the network signal strength, it will invoke a callback whenever the signal strength changes [10].

• *getAllCellInfo().* : is another way to get the network signal strength is to make an explicit call to the operating system by invoking the *getAllCellInfo()* method (available under the *TelephonyManager* class) to fetch the most recent signal strength known to the hardware [11].

The two methods are supposed to report the change in the signal strength of the network. But what about their performances? Do they have the same sensitivity? Which one is better to monitor the changes in the signal strength?

In order to compare the performance of the two methods available on Android to get the received power, we put an LG Nexus 5X smartphone at the reception side of the anechoic chamber in front of a source, as shown in Figure 3. Then, we vary the transmission between -45 dBm and -20 dBm with a step of 1 dB every minute. We record the received power on the smartphone using the two aforementioned methods. We trigger a call to *getAllCellInfo()* every 1 second. The results are shown in Figure 5.

The method *getAllCellInfos()* is more sensitive to the change in the received signal than the *PhoneStateListener* method. For example, at time 10h45, *PhoneStateListener* keeps giving the same power (-80 dBm) regardless of dropping the transmission power from -20 dBm to -25 dBm, then it suddenly updates to -85 dBm.

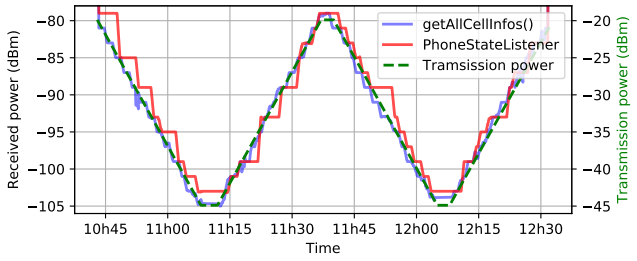

Figure 5: Comparing Android API calls to get the cellular received power. *getAllCellInfos()* method is more reliable and more sensitive to change in the signal strength than the *PhoneStateListener* method.

In contrast, *getAllCellInfos()* follows exactly the updates in the transmission power.

For the rest of this work, we choose *getAllCellInfos()* to measure the received power on the smartphone.

3.4.2 Getting the smartphone orientation on Android. The orientation of the smartphone is obtained using another Android APIs, called Rotation Vector Sensor (RVS). It is a software sensor that combines many hardware sensors readings (Accelerometer, Magnetometer, and Gyroscope) to estimate the device's orientation in space. The RVS, as its name suggests, returns a vector from which we can extract a normalized quaternion of orientation. Quaternion[9] is a mathematical representation of orientation. Quaternions are 4 dimensional complex vectors in a form of $a + bi + cj + dk$, where a is the real part of the quaternion. Quaternions can be averaged by interpolation, known as slerping [9] (Spherical Linear intERPolation) and, in contrast to Euler angles, they do not suffer from Gimbal lock, which is a loss of a degree of freedom to represent the orientations in a three-dimensional space [3].

The program that controls the two-axis positioner generates logs containing each axis angle (in degrees) of both the reception and transmission positioners. A separate text file is created for every programmed orientation with a corresponding timestamp. These logs are solely used as ground truth values for device orientation inside the chamber and also to group the smartphone logs for each programmed orientation.

3.5 Experimental limitations

For measurement acquisition, we faced some limitations.

First, the received signal strength from the smartphone does not have a high refresh rate (around 1 second at best). It is due to power optimization by restricting the number of messages exchanged between the device's baseband (which has a higher refresh rate) and the Android OS.A higher refresh rate would have shortened the time spent on collecting the calibration data.

Second, the two-positioner system can only rotate along two axis, which means we cannot test all the relative orientation of the device with respect to the source. This can be solved by rotating the source itself along φ. We limit our study on a subset of relative orientations of the smartphone to the source by considering two polarizations of the source (horizontal and vertical polarization), and all the details of the calibration process we present in this work can be replicated on any other orientations or polarizations without loss of generality.

4 EVALUATING THE EFFECT OF ORIENTATION ON THE RECEIVED POWER

In this section, we evaluate the accuracy of the smartphone's raw measurements of signal strength inside an anechoic chamber for a mono-polarized antenna and quantify the effect of smartphone's orientation with respect to the source on the received power.

4.1 Measuring the reference power

First, we measured the real RSSI power at the reception using a Rohde-Schwarz FSL3 spectrum analyzer [29]. We use a horizontal polarization at the source. We mount on the spectrum analyzer a horn antenna identical to the transmitting antenna with the same polarization as the source. By removing the antenna gain (10 dB) and compensating for cable loss (1 dB), the power measured at the reception is **-54 dBm**. We call this power *the reference power*.

4.2 Sensitivity to orientations

We want to know how close the RSSI power measured by a COTS smartphone is from the reference RSSI power. To do so, we replace the horn antenna at reception with a smartphone. In order to study the effect of the smartphone orientation on the received power, we put the device in different orientations in space along two axis: φ and θ directly in front of the transmitting antenna, as illustrated in Figure 3. At each position, we collect the received power and the device orientation.

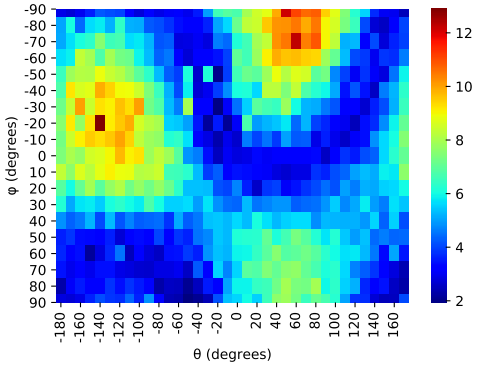

Figure 6: Mean angle error (in degrees) in all 684 orientations. Overall, the error is very low and less than 10 degrees in most orientations. Few orientations give more than 10 degrees error.

We keep the device at each orientation for 10 seconds, this allows the mobile application to collect about 10 tuples of (orientation, power). We then average these tuples into one tuple of (power, orientation). Power averaging is done in a linear scale (Watt) and the result is converted back to the logarithmic scale (dBm). The orientation is obtained by slerping quaternions and expressed as a normalized quaternion with magnitude equals to 1 to represent the smartphone orientation in space in order to keep track of the effect of orientation on the received power.

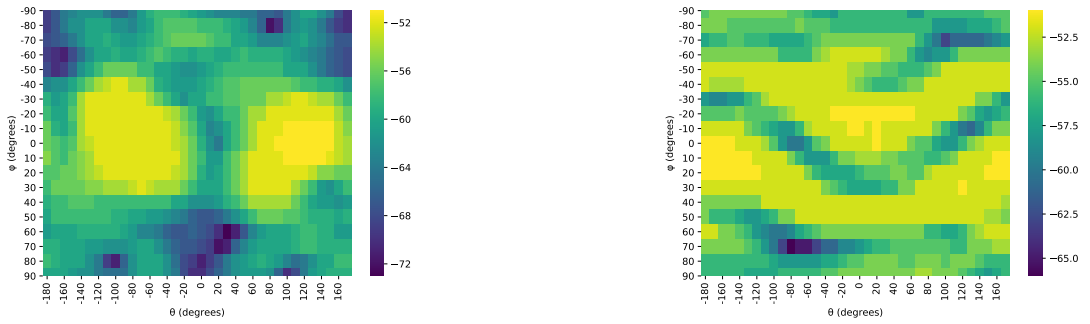

(a) H-polarization

(b) V-polarization

Figure 7: Heatmap of received signal strength (in dBm) by the LG Nexus 5X for 684 orientation with two polarization of the source (a) For Horizontal polarization, the maximum received power is -70 dBm, which is 16 dB below the reference power, and variability of the received power up to 24 dB between minimum and maximum received power. (b) For Vertical polarization, we observe a a maximum power of -68 dBm and an offset of 18 dB between maximum and minimum received power.

To verify the stability of the received power at each orientation during the 10 seconds of measurements, we calculated the standard deviation of power at each orientation. The mean standard deviation of powers in all the 684 orientation was only 0.06 dBm.

Moreover, to verify the reproducibility of the measurements in the controlled environment, we repeated the same experiment 10 times. For every experiment, we start the experimental process from scratch: we set up the cellular network, we calibrate the orientation sensors smartphone [7], we position it on the two-positioner system, then launch the controller program to start rotating the device and collect the measurements. We computed the mean standard deviation of the received power at each orientation in all experiments is 0.51 dBm. We also computed the mean angle error for each orientation in the 10 experiments. The results are depicted in Figure 6. Overall, we have a mean angle error of 5.5 degrees. The error varies depending on the orientation. Most orientations have low angle error and few of them have up to 13 degrees. The angle error is due to the accuracy of the hardware sensors embedded on the device, which could be impacted by the quality of the sensors or any electromagnetic interference from the anechoic chamber apparatus's motors. However, we consider this level of precision good enough for our study.

We merged all 10 experiments and for each orientation, we compute the average power and the mean quaternion using quaternion slerping. For the rest of our study, we consider using the resulting averaged powers and orientations.

Figure 7 (a) shows a heatmap of the resulting received signal power in all 684 orientations with horizontal polarization of the source.

We clearly see the variability of the received signal strength between different orientations. The optimal power we measured was -51 dBm at θ = +90 and φ = 0 (same orientation as depicted in Figure 3), which is 3 dB more than the reference power (-54 dBm). This difference can be due to the smartphone antenna gain. At some orientations, the performance of the receiving antennas is very poor with a minimum of -73 dBm.

We evaluated another polarization of the source (vertical polarization) by repeating the same measurement process performed for the horizontal polarization. The resulting received power for the same 684 orientations are shown in Figure 7 (b). Again, we see the variability of received power with an offset of 15 dBm between the maximum and the minimum received power by the smartphone. These results are expected given the small size of smartphone antennas and their design in addition to the smartphone casing. *Hence, the smartphone cannot precisely measure the real power out-of-the-box.*

For the rest of this work, we consider only the horizontal polarization of the source. The study can easily be replicated to any other polarization without loss of generality.

Next, we explore the orientations that minimize and maximize the received power. In antenna theory, *Polarization Matching* [6] (or co-polarization) means that the receiver and transmitter have the same polarization, and the power loss is minimal. In contrast, cross-polarization yields minimal power. To verify whether we can detect polarization matching and cross-polarization with smartphones, we plotted the mean received power along the two axes of rotation in Figure 8. Along φ axis, the maximum power is received when the smartphone is in the main lobe of transmission (φ = 0). We also see that the maximum power along θ is at +120 degrees and -60 degrees, and lowest when the smartphone is rotated by 90 degrees along θ. Hence, smartphone antennas are affected by their relative orientation with respect to the source and the optimal performance is observed when its polarization matches the polarization of the source.

In conclusion, *COTS smartphone measurements of the received power can be affected by the orientation of the smartphone in space.* In the next section, we mitigate these two issues by calibrating the received power, that is, obtaining a measured power close to the real power and independent from the smartphone orientation.

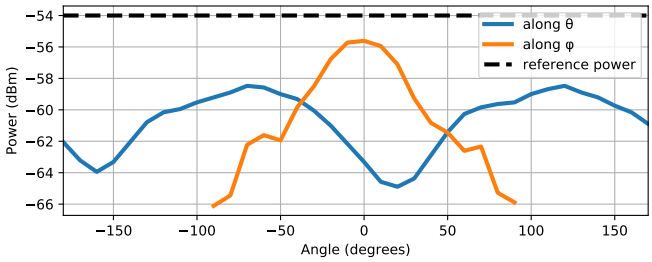

Figure 8: Mean received power along φ and θ. The received power is optimal when the antenna is in co-polarization with the source (θ = 120 and θ = -60) and when the smartphone is directed towards the source (φ = 0)

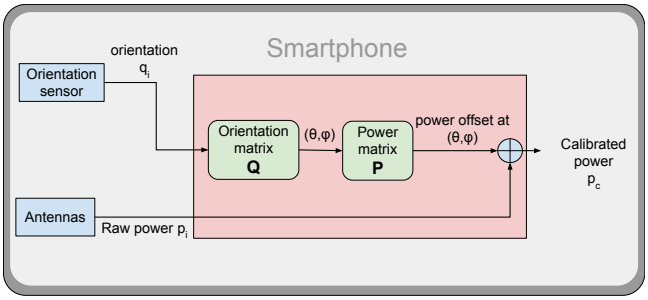

Figure 9: Calibration process. The smartphone measures the power p_i and the orientation q_i. From Q we find the closest calibrated orientation and its coordinates (θ, φ), P gives us the corresponding calibration offset at the same coordinates, which is then added to the raw power p_i to get the real power.

5 CALIBRATION

5.1 Calibration technique

In order to calibrate the received signal strength, we make use of the embedded sensors of the smartphone to capture the orientation in space combined with the raw received power. The idea is to make lookup tables or matrices for orientations and power, from which we determine the correcting factor to apply at a given orientation.

Let Q be a matrix of orientation Quaternions, and let P, another matrix having the same dimensions as Q, be a matrix of Power. We call them calibration matrices. We rotate the smartphone as shown in Figure 3. For each orientation, we fill up the matrix Q with the measured quaternion, and the matrix P with the offset between the raw measured power at that orientation and the reference power we measured beforehand in section 4.1 using the spectrum analyzer. In other words, each cell in the matrix Q contains a quaternion representing a given orientation. In each cell of matrix P, we put the difference between the reference power and the raw measured power at the orientation described by a quaternion in Q at the same coordinates. The calibration process is summarized in Figure 9.

Once we have these two matrices, whenever we put a device in a given orientation defined by a quaternion q_i, we compare it to every quaternion in Q and compute the relative angle. The closest quaternion in Q gives us the minimal angle. We use its coordinates in Q to obtain the corresponding correction offset from P to apply it on the raw measured power in order to calibrate it.

Performance-wise, quaternion lookup and comparison in Q has linear complexity. The performances can be improved by using hashing data structures for faster lookup. For this work, we settle for the linear approach and consider the optimization in future works.

5.1.1 Building the calibration matrices P *and* Q. The first step is to build the calibration matrices and use them as lookup tables to determine which correction offset to apply on the received power. To do this, we rotate the smartphone as depicted in Figure 3. We initially put the device at θ = -180, and φ = -90. Then, we move θ from -180 degrees to +170 degrees with steps of 10 degrees. We do that for every φ that goes from -90 to +90 with a step of 10 degrees. At each step, we collect the received power and rotation quaternion. Then, we insert them in the matrices with the corresponding φ and θ coordinates. The dimensions of the matrices P and Q will be a 36x19 matrices.

5.1.2 Post processing. At the end of each experiment, we obtain the smartphone logs containing the received power, the rotation quaternions, and their timestamps. We also extract the generated logs of the rotating apparatus of the anechoic chamber containing the exact orientation of the reception platform (hence, the smartphone) and the timestamp it reached this orientation. The apparatus logs record the values of φ and θ which are used as coordinates when filling the calibration matrices. The apparatus logs also contain timestamps which are used to filter the smartphone logs for each orientation.

We put all log files in one folder then run a script we wrote that reads, extracts and filter the logs to generate the two calibration matrices, P and Q.

5.2 Calibration

Now that we obtained the calibrating matrices, can we calibrate any other random orientations? To test this, we generated 100 random orientation by taking 10 random values for φ and θ in the ranges [90,+90] and [-180, 170] respectively in such a way that the random orientations are not in Q. The source polarization and transmission power are kept unchanged.

The received power and the orientation are collected and processed as explained in section 4.2.

The calibration is applied as follows: for every random orientation, we compare the corresponding quaternion to every quaternion in Q to get the closest quaternion and its coordinates. We use these coordinates to determine the power offset to add to the measured power to calibrate it. The calibration process is summarized in Figure 9.

Applying this process on the 100 random orientation gives the results depicted in Figure 10. The calibrated power is very close to the reference power measured by the spectrum analyzer, as opposed to the raw measurement, which feature a high variability and can be much below the reference power. To quantify the quality of the calibration, we use the Root Mean Square Error (RMSE) between the calibrated signal and the reference power. RMSE is defined in

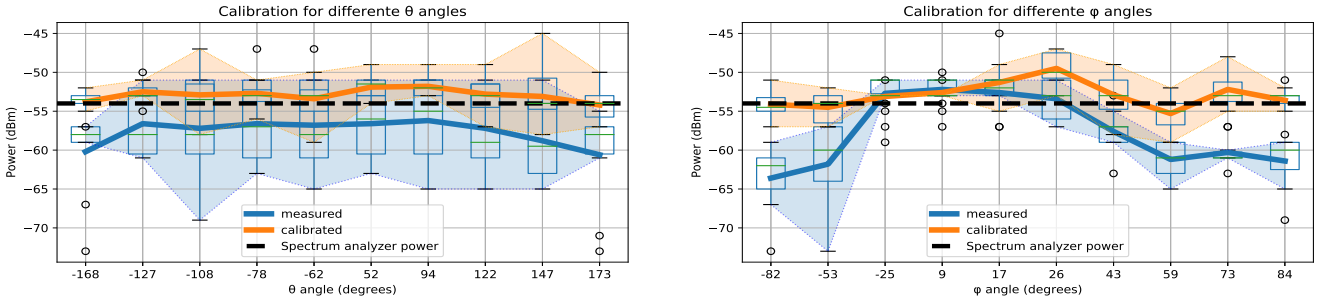

Figure 10: Boxplots for calibration results of the 100 random orientations along θ and φ. The calibrated signal (orange) is closer to the reference power (black dashed line), and less variable compared to the raw measured signal (in blue). The colored area represents the variability range of measurements. The RMSE for the calibrated values is 2.4 dBm compared to 6.4 dBm error for the raw measurements.

Equation 1.

$$\text{RMSE} = \sqrt{\frac{\sum_{i=1}^{N} \left(P_{\text{ref}} - P_{i,\text{calibrated}}\right)^2}{N}} \tag{1}$$

Where N in Equation 1 represents the number of orientations we tested (In this case, N = 100).

The RMSE for the calibration is only 2.4 dBm compared to 6.4 dBm RMSE for non-calibrated measurements. This shows that our calibration process gives satisfying results that compensate for smartphone antenna performances and the effect of orientation on the received power.

6 ADAPTING CALIBRATION FOR UNKNOWN SOURCE CHARACTERISTICS

In section 5, we studied the effect of device orientation in space on the received signal strength. We showed how we can calibrate the measurements to compensate for this effect. Up to now, the location of the source is supposed to be known. What will happen if the source is moved, or the transmission power is changed? Can we find the new location of the source and reuse the calibration matrices obtained before?

In this section, we evaluate our calibration technique against a change in the transmitted power or a change of the source location with respect to the smartphone. Then, we verify to which extent the calibration matrices are still valid. To simplify the study, we assume that the source polarization does not change and is known beforehand, knowing that we can still estimate the polarization using the property of polarization matching, as explained in section 4.2. Without loss of generality, we only consider changing the source location along the azimuth axis (θ).

6.1 Calibration for aligned source with unknown position

Now, let's consider the case where the source's location with respect to the smartphone is unknown. How does this affect the received pattern of the smartphone and how can we calibrate a signal coming from an unknown direction? In this experiment, we put the transmitting antenna at different azimuth (φ) angles around the smartphone while keeping the smartphone inside the main lobe of transmission. We then test whether we can reuse again the calibration matrices to calibrate the received power.

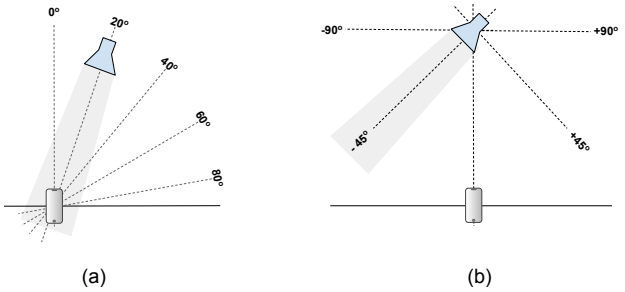

Figure 11: (a) Changing the source's position with respect to the smartphone. **(b)** Pointing the source's main lobe at different angles with respect to the smartphone.

As shown in Figure 11 (a), we rotate the source at 20, 40, 60 and 80 degrees from the original orientation. We precisely position the source using a laser beam and axis value readings from the rotating apparatus of the anechoic chamber to make sure that the source is shifted by the correct angle. At each new position, we measure the reference power using a spectrum analyzer.

Figure 12 shows the received power patterns for all the tested angles. The patterns seem to be a shifted version of the reception pattern at 0 degrees. To verify and validate this, we make a correlation plot between them and the measured pattern at 0 degrees. This is shown in Figure 13. We see that the reception patterns are highly correlated at exactly 20, 40, 60 and 80 degrees shift with respect to the measurements at 0 degrees. Hence, the reception pattern is preserved regardless of the source position with respect to the smartphone.

Now that we showed the preservation of the reception pattern even if we move the source and change its location, it means we can reuse the calibration matrices we collected when the source was at φ=0 degrees in order to calibrate the received power when the source is at different angles with respect to the smartphone. To do so, we first need to locate the new position of the source, then define the angle shift from φ=0 position to the new source position.

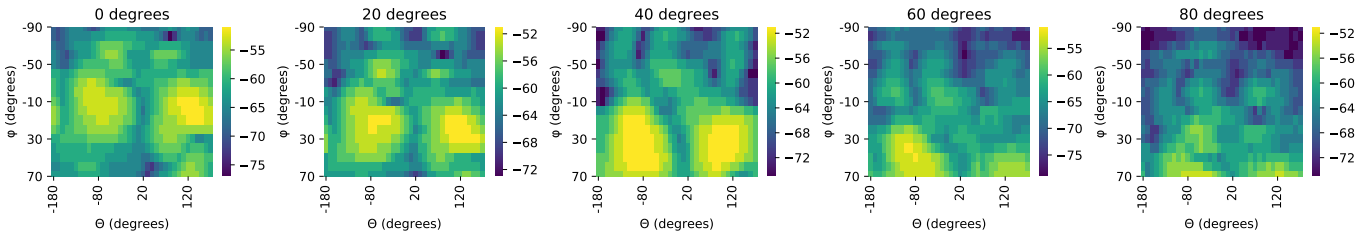

Figure 12: The received power by the Nexus 5X when the source is put at different angles. The reception patterns are a shifted versions of pattern at 0 degrees with the corresponding angle change in source position.

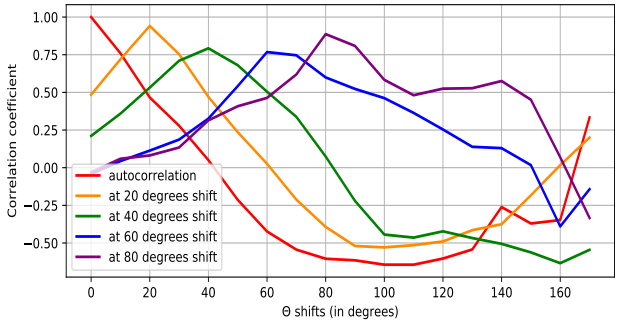

Figure 13: Correlation plots. The reception patterns are highly correlated with the pattern at 0 degrees with shifts corresponding to the new source position.

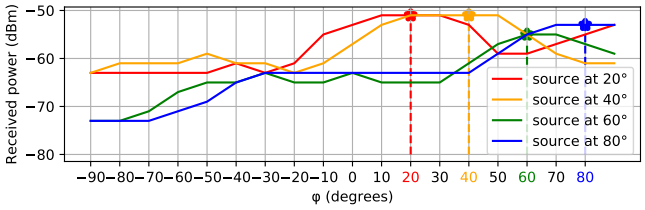

Figure 14: Sweeping along φ axis to locate the source. The Source is located where the maximum power is measured.

Then, we translate the calibration matrix of orientation Q to adapt it to the new source position.

To locate the source, we use the property of antennas polarization we explained in section 4.2, where the reception is maximum when both the transmitting and the receiving antennas are aligned and co-polarized, i.e., they have the same polarization. So, by knowing the polarization at transmission, we put the smartphone in the same polarization, then we sweep along φ and collect the received power. The source will be located when we measure the maximum power at an angle $\varphi = \varphi_m$.

The smartphone receives more power when θ is +120 or -60 degrees, as illustrated in Figure 8. So we put the smartphone at $\theta = 120$, then we rotate the phone along φ axis from -90 degrees to +90 degrees and collect the received power at each value of φ. The results are plotted in Figure 14. The received power increases gradually as we point the smartphone closer to the new source location. The maximum power is received when the smartphone is directly aligned with the source along the azimuth (φ).

After we locate the source, we need to transform and shift the matrix of orientation quaternions Q to adapt it to the new source change. We apply quaternion rotation using the relative quaternion describing the rotation from $\varphi = 0$ to $\varphi = \varphi_m$, the new source position in the azimuth.

Now that we adapted the calibration matrices to the change in source position, we can calibrate the received power. The RMSE between the calibrated and the reference power are plotted in Figure 16(a) for all tested source positions. The RMSE is below 5 dBm in all cases. *We conclude that we can calibrate the smartphone measurements from a source with unknown location along the azimuth.*

6.2 Calibration outside the main lobe of transmission of a source with known position

Previously, we considered the calibration when the source position or transmission power is unknown and the smartphone was in the main lobe of transmission of the source. What will happen to the received signal power when the smartphone is no more inside the main lobe? Can we still calibrate in that case?

In this section, we study the received power when the smartphone is not directly targeted by the main lobe of the transmitting antenna. As shown in Figure 11 (b), we point the main lobe at different angles with respect to the smartphone, At each angle, we rotate the smartphone along φ and θ to collect the received power.

Figure 15 shows the heatmap of the received power by the smartphone in all tested cases.

Now, can we still reuse the calibration matrices P and Q to calibrate the received power when the source's main lobe is not directed towards the smartphone?

We apply the calibration process described in Section 5.1 for each case of source rotation. First, we measure the reference power with a spectrum analyzer, then we put the device in the same 684 orientations and apply our calibration matrices P and Q to calibrate the measurements.

The RMSE for the calibrated signals in all cases are shown in Figure 16(b). Again, we see that the RMSE is within 5 dBm. *This shows that the calibration still works even if the smartphone is not directly in the main lobe of transmission.*

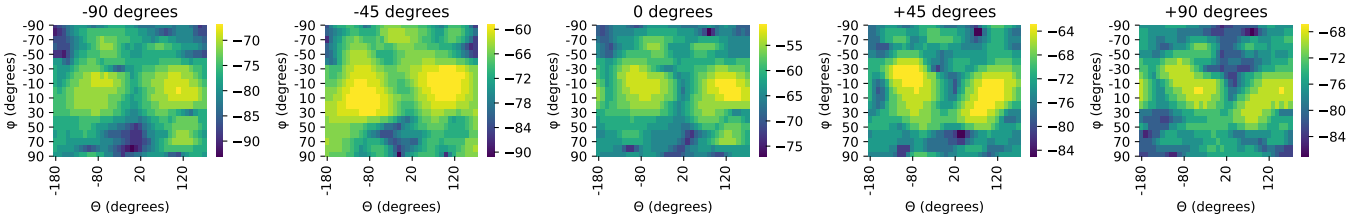

Figure 15: Heatmap of the received pattern by the Nexus 5X when the main lobe is oriented in different direction.

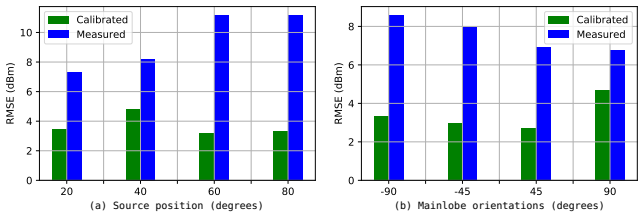

Figure 16: Calibration RMSE for unaligned source

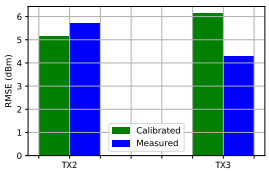

Figure 18: Calibration RMSE for different transmission power

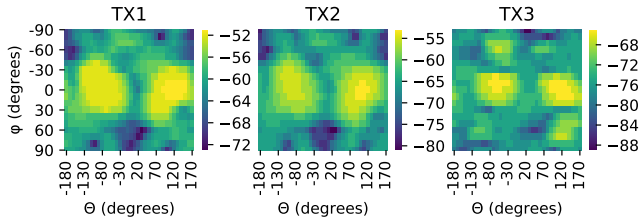

Figure 17: The received power by the Nexus 5X for different transmitted power

6.3 Calibration for unknown transmission power

The last case we considered is a change in the transmitted power. The position of the source and its polarization are kept the same as shown in Figure 3. We reduced the transmitted power twice with 10 dB difference each time by changing the transmission attenuation parameter `att_tx` found in the configuration file of OAI. We obtain three different powers (TX1, TX2, and TX3). For each transmitted power, we measure the reference received power as explained in section 4.1. We measure -54 dBm, -64 dBm, and -74 dBm for TX1, TX2, and TX3, respectively. For each transmitted power, we collect measurements with the same process as described in section 5.1 by rotating the smartphone along θ and φ. The resulting received patterns for all the different transmitted powers are depicted in Figure 17.

We tried to apply the same calibration matrices P and Q for the two changes in the transmitted power. We computed the RMSE in each situation. The results are shown in Figure 18. We see that the calibration didn't improve much for the case of TX2 and it worsened the RMSE for TX3.

Changing the transmitted power affected the reception patterns of the smartphone. Indeed, in LTE, smartphones work with a Multiple Input Multiple Output (MIMO) technology. Depending on the network quality, the smartphone can select a single antenna or combine the different antennas to optimize the received signal power [12]. This is called antenna diversity.

There exist different techniques for diversity combining [19]. The smartphone may use only one of the antennas for reception (switched diversity) or combine the incoming signal from all antennas according to their respective Signal-to-Noise Ratio (SNR) such as Maximum Ratio Combining (MRC).

This antenna diversity significantly complicates the calibration process as we have no a priory knowledge of which calibration matrix must be used for the measured received power.

To deal with this issue, we evaluate the performance of a machine learning model (Random Forrest) to predict the correct received power. We consider two cases. First, we consider a model in which we label with the reference received power a single random point in the calibration matrices presented in Figure 17. A point consists of the tuple (measured received power from the device, device orientation). Second, we consider a model in which we label two random points (taken from the same matrix) with the reference received power.

To perform the evaluation, we train the model with X% of the points, X ranging from 5% to 97% by step of 4. The remaining set of points are used for the validation. For each X, we repeat the training 10 times with another uniformly distributed random subset of X% of the points each time. The accuracy of the model to give the correct received power is shown in Figure 19.

We see that with 30% of training data, the model can predict with 90% accuracy the reference received power with a single point of measure. The accuracy jumps to 95% if we use two points of measure. Even more striking, with only 5% of training data the accuracy is 80% for a single point of measure.

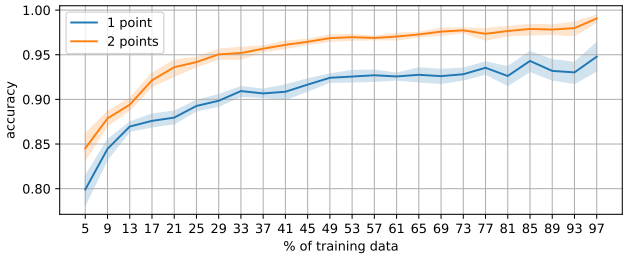

Figure 19: Random Forrest accuracy for selecting the right reception power for different amounts of training data. The line represents the average over 10 independent training, and the colored shape represent the 95% confidence interval.

Figure 20: Interior of sector antenna (MIT Computer Science & Artificial Intelligence Lab). An array of dipole antennas in a "+" configuration to transmit the same signal on two perpendicular polarizations in order to minimize polarization mismatch at reception. Hence, improves cellular reception.

This means that a simple random forest model can capture from a single measurement point the reference received power with high accuracy even with a small amount of training data. So we can calibrate with such a model measures performed with different antenna diversity optimizations.

7 SIGNAL STRENGTH ACCURACY WITH A MULTI-POLARIZED ANTENNA IN AN OUTDOOR ENVIRONMENT

So far, we studied the received signal strength accuracy of a smartphone in a controlled environment with a mono-polarized emitting antenna. In this section, we evaluate the accuracy of the RSSI with a multi-polarized antenna in an outdoor environment that is more dynamic with many reflections and multipath effects. Moreover, the base stations nowadays use transmission diversity, like spacial diversity and polarization diversity where the signal is transmitted at two perpendicular polarizations from an antenna array in order to improve cellular reception. Polarization diversity gives a gain of up to 12 dB compared to single polarization [16]. A typical sector antenna's interior used at the base stations is depicted in Figure 20.

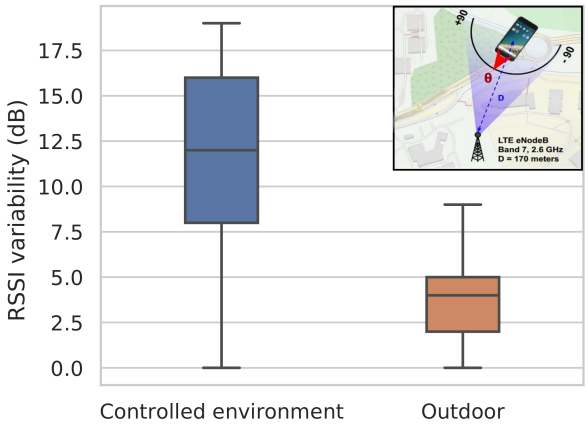

Figure 21: Outdoor evaluation. The smartphone measurements outdoor are much less affected by the orientation compared to the measurements collected in a mono-polarized, controlled environment, evaluated on the same 88 different orientation with respect to the source.

We can clearly see the arrangement of multiple antennas with vertical and horizontal alignment. They are used to transmit the same signal on two perpendicular polarizations in order to minimize polarization mismatch at reception.

To assess the accuracy of the RSSI measurement from a smartphone in these conditions, we put the LG Nexus 5x smartphone, that we used in our study, in 88 different orientations (which are a subset of the 684 orientations we tested in the controlled environment) inside the main lobe of transmission of an LTE base station, at a distance of 170 meters, see Figure 21. The direction of the main lobe is obtained from the official maps provided by the French national agency of radio-frequencies (ANFR) [8]. We locked the smartphone on the same band we used in the controlled environment, band 7. The orientations are again described in terms of φ and θ. We distributed the 88 orientations on the two axes φ and θ to test different relative orientations between the smartphone and the source. At each orientation, we collected at least 20 measurement samples of the received power. We computed the variability of the measurements collected outdoor, and we compare it to the variability of measurements collected in the controlled environment with a mono-polarized source, at the same set of orientations. The results are shown in Figure 21.

The measurements collected outdoor are less variable than what we obtained in the controlled environment. The median variability is about 4 dB outdoor, compared to 12 dB in the controlled environment.

By transmitting the same signal at two perpendicular polarizations (vertical and horizontal polarizations), the smartphone antennas can compensate the errors introduced by the radiation patterns by combining signals from multiple antennas more efficiently. So the polarization diversity used at transmission minimizes the chance of polarization mismatch (or cross-polarization). Hence, the effect of orientation on the received power in an outdoor environment is minimized (low directivity), and *smartphones can be*

used outdoor for wireless power measurement with less than 4 dB variability.

8 DISCUSSION

In this work, we evaluated the accuracy of the received signal strength from a 4G antenna with a commercial off-the-shelf (COTS) smartphone. We considered both a mono-polarized and a multi-polarized antenna as the source of the signal. We have shown that a mono-polarized antenna leads to high inaccuracy due to the smartphone orientation, source position, and source power, but that we can calibrate the RSSI to obtain a value close to the reference power measured with a professional equipment.

In the case of the multi-polarized antenna, we have shown that the measured RSSI is not sensitive to the device orientation.

This work raises two main questions that we discuss in the following.

Do our results hold for other types of devices? We replicated the calibration process with 6 additional devices, a Samsung S4, S5, S7, a Nexus 6, a Pixel 2, a Note 4 (not shown due to space limitation). Therefore, we are confident that our results can be generalized to many smartphones.

Do our results hold for other kinds of wireless technologies? The calibration matrices we produced are specific to the antennas used in the smartphone for LTE. However, most of our results provide a strong basis for other wireless technologies. For instance, our methodology can be reused for 2G and 3G cellular protocols that use multi-polarized antennas. On the contrary, Bluetooth is using mono-polarized antennas. We validated experimentally in our anechoic chamber environment that the Bluetooth RSSI measured from our Nexus 5X is highly sensitive to the orientation of the device with 22 dBm of variability. This is a critical problem for positioning solutions that rely on the RSSI to find the position of a device with Bluetooth beacons [31][17]. The calibration techniques we developed can be reused in this context to improve Bluetooth distance estimations.

In conclusion, surprisingly, estimating the RSSI for a COTS smartphone is a difficult problem with several important practical applications such as estimating the cellular coverage of an operator for cellular infrastructure optimizations, estimating the exposure of the population to different wireless technologies for epidemiological studies, or estimating the RSSI of Bluetooth beacons for accurate indoor positioning.

We believe that this work makes a step forward in establishing a methodological framework to improve the accuracy of RSSI measurements from COTS smartphones.

REFERENCES

[1] Evolved Universal Terrestrial Radio Access. [n.d.]. Physical layer—Measurements (3GPP TS 36.214 version 9.1. 0 Release 9)". *ETSI TS* 136, 214 ([n. d.]), V9.

[2] Andreas Achtzehn, Janne Riihihjärvi, Irving Antonio Barriía Castillo, Marina Petrova, and Petri Mähönen. 2015. CrowdREM: Harnessing the power of the mobile crowd for flexible wireless network monitoring. In *Proceedings of the 16th International Workshop on Mobile Computing Systems and Applications*. ACM, 63–68.

[3] A Alaimo, V Artale, C Milazzo, and A Ricciardello. 2013. Comparison between euler and quaternion parametrization in uav dynamics. In *AIP Conference Proceedings*, Vol. 1558. AIP, 1228–1231.

[4] XMobiSense app. 2020. http://www.thecosmosproject.org/xmobisense-app [Online; accessed 31. Jan. 2020].

[5] Robert Baan, Yann Grosse, Béatrice Lauby-Secretan, Fatiha El Ghissassi, Véronique Bouvard, Lamia Benbrahim-Tallaa, Neela Guha, Farhad Islami, Laurent Galichet, and Kurt Straif. 2011. Carcinogenicity of radiofrequency electromagnetic fields. *The Lancet Oncology* 12, 7 (2011), 624 – 626. https://doi.org/10.1016/S1470-2045(11)70147-4

[6] Constantine A Balanis. 2016. *Antenna theory: analysis and design*. John wiley & sons.

[7] calibrateMag. 2019. *Calibrating magnetometer sensor*. ww2.mathworks.cn/help/supportpkg/beagleboneblue/ref/calibratemag.html

[8] Cartoradio - ANFR. 2020. https://www.cartoradio.fr/ [Online; accessed 3. Feb. 2020].

[9] EB Dam, M Koch, and M Lillholm. 1998. Quaternions Interpolation and Animation. Datalogisk Institut. *Københavns Universitet* (1998).

[10] Android Developers. 2019. *PhoneStateListener*. https://developer.android.com/reference/android/telephony/PhoneStateListener

[11] Android Developers. 2019. *TelephonyManager*. https://developer.android.com/reference/android/telephony/TelephonyManager.html#getAllCellInfo()

[12] Carl B Dietrich, Kai Dietze, J Randall Nealy, and Warren L Stutzman. 2001. Spatial, polarization, and pattern diversity for wireless handheld terminals. *IEEE transactions on antennas and propagation* 49, 9 (2001), 1271–1281.

[13] ElectroSmart. 2020. https://electrosmart.app [Online; accessed 31. Jan. 2020].

[14] Ettus. 2019. *Ettus USRP B210*. www.ettus.com/product/details/UB210-KIT

[15] International Agency for Research on Cancer. 2020. The Interphone Study. http://interphone.iarc.fr [Online; accessed 31. Jan. 2020].

[16] Kyōhei Fujimoto. 2001. *Mobile antenna systems handbook*. Artech House.

[17] Yu Gu and Fuji Ren. 2015. Energy-Efficient Indoor Localization of Smart Hand-Held Devices Using Bluetooth. *IEEE Access* 3 (Jun 2015), 1450–1461. https://doi.org/10.1109/ACCESS.2015.2441694

[18] Sampson Hu and David Tanner. 2018. Solving the antenna paradox: Adding more antennas to your smartphone creates more noise, but 3D manufacturing will fix the problem. *IEEE Spectrum* 55, 11 (2018), 40–45.

[19] Sukhdeep Kaur, Jaipreet Kaur, and Manjit Sandhu. [n.d.]. Antenna Diversity Techniques. ([n. d.]).

[20] Application name removed to preserve anonymity. 2020.

[21] Ana Nika, Zengbin Zhang, Xia Zhou, Ben Y Zhao, and Haitao Zheng. 2014. Towards commoditized real-time spectrum monitoring. In *Proceedings of the 1st ACM workshop on Hot topics in wireless*. ACM, 25–30.

[22] Navid Nikaein, Raymond Knopp, Florian Kaltenberger, Lionel Gauthier, Christian Bonnet, Dominique Nussbaum, and Riadh Ghaddab. 2014. OpenAirInterface: an open LTE network in a PC. In *Proceedings of the 20th annual international conference on Mobile computing and networking*. ACM, 305–308.

[23] OpenSignal. 2020. Mobile Analytics and Insights | Opensignal. https://www.opensignal.com [Online; accessed 31. Jan. 2020].

[24] CORDIS project. 2020. Final Report Summary - EMF-NET (Effects of the exposure to electromagnetic fields: from science to public health) | Report Summary | FP6 | CORDIS | European Commission. https://cordis.europa.eu/project/id/502173/reporting/fr [Online; accessed 31. Jan. 2020].

[25] GERONIMO Project. 2020. Generalised EMF Research using Novel Methods – an integrated approach: from research to risk assessment and support to risk management | GERONIMO Project | FP7 | CORDIS | European Commission. https://cordis.europa.eu/project/id/603794 [Online; accessed 31. Jan. 2020].

[26] OpenMoko project. 2019. *OpenMoko*. www.openmoko.org

[27] OsmocomBB project. 2019. *OsmocomBB*. osmocom.org/projects/baseband

[28] The COSMOS project. 2020. http://www.thecosmosproject.org [Online; accessed 31. Jan. 2020].

[29] Rohde&Schwarz. 2019. *FSL3 Spectrum Analyzer*. www.rohde-schwarz.com/fr/produit/fsl-page-de-demarrage-produits_63493-8042.html

[30] Tutela. 2020. https://www.tutela.com [Online; accessed 31. Jan. 2020].

[31] Yixin Wang, Qiang Ye, Jie Cheng, and Lei Wang. 2015. RSSI-based bluetooth indoor localization. In *2015 11th International Conference on Mobile Ad-hoc and Sensor Networks (MSN)*. IEEE, 165–171.

[32] Tan Zhang, Ashish Patro, Ning Leng, and Suman Banerjee. 2015. A wireless spectrum analyzer in your pocket. In *Proceedings of the 16th International Workshop on Mobile Computing Systems and Applications*. ACM, 69–74.